STUDY OF THE NULL DIRECTIONS ON THE PERFORMANCE OF DIFFERENTIAL BEAMFORMERS

Xuehan Wang[1,2]*, Israel Cohen*[2]*, Jacob Benesty*[3]*, and Jingdong Chen*[1]

[1]CIAIC and Shaanxi Provincial Key Laboratory of Artificial Intelligence,
Northwestern Polytechnical University, Xi'an, Shaanxi 710072, China
[2]Andrew and Erna Viterbi Faculty of Electrical & Computer Engineering
Technion – Israel Institute of Technology, Technion City, Haifa 3200003, Israel
[3]INRS-EMT, University of Quebec, Montreal, QC H5A 1K6, Canada

ABSTRACT

Null directions are important parameters for differential beamformers, which play an important role on the beamforming performance. In this paper, we investigate the performance of differential beamformers as a function of the null directions. We first derive the directivity factor (DF) as an explicit function of null and show that the DF decreases to 0 if any null approaches to the desired look direction. We then validate the theoretical analysis through simulations using the beampattern, DF and signal-to-interference gain as the performance measures. The results show that: 1) the performance of a differential beamformer degrades significantly if there is any null close to the desired look direction; 2) with a fixed null direction, increasing the order of the differential beamformer can help improve performance.

***Index Terms*—**Differential beamforming, microphone array, directivity factor, interference suppression.

1. INTRODUCTION

In many speech related applications such as teleconferencing and human-machine interfaces, microphone arrays have to be used to extract the speech signal of interest from its observations contaminated by ambient noise, interference and reverberation. The most critical part of a microphone array system is the so-called beamforming, which takes the array observations as its inputs and generates an estimate of the signal of interest exploiting the redundancy among the multichannel observation signals [1–5]. Over the past several decades, a large number of beamforming algorithms have been developed [6–9], among which the differential beamforming (the resulting array is called a differential microphone array, or simply a DMA) has attracted much interest because such a method can produce frequency-invariant spatial responses and have the potential to obtain high directivity with compact array apertures [10–20].

Conventionally, the differential beamformer is designed in a cascaded structure, i.e., an Nth-order differential beamformer is formed by subtractively combining the outputs of two $(N-1)$th-order differential beamformers [21]. To better deal with the problem of white noise amplification, which is inherent to differential beamforming, a null-constrained method was developed [10,22], which was motivated by the facts that the ideal beampattern of an Nth-order differential beamformer has at most N nulls [10, 22, 23]. It converts the beamformer design problem into one of linear system identification where the linear system is constructed using the information from the desired look direction as well as the nulls. A minimum-form solution of the linear system can help improve the white noise gain (WNG) by increasing the number of microphones, thereby improving the robustness of the beamformer [10, 11, 24, 25]. Apparently, the null positions play an important role on the performance of differential beamformers, the analysis of which is the focal point of this work.

To study how a null may affect the performance of a differential beamformer, we first express the Nth-order ideal differential beampattern as an explicit function of the null. We then investigate the relationship between the null direction and the level of directivity factor (DF). Through this relationship, we show that for any order of differential beamformer, the DF will decrease significantly if there is a null approaching the look direction. To further validate the analysis, simulations are performed. The results show that the effectiveness of beampattern, null depth, DF and the level of interference suppression all suffer from significant degradation as the null direction approaches the desired look direction, which corroborates the theoretical analysis.

2. SIGNAL MODEL, PROBLEM FORMULATION AND PERFORMANCE MEASURES

Consider a farfield plane wave that propagates in an anechoic acoustic environment at the speed of sound, i.e., $c = 340$ m/s, and impinges on a uniform linear microphone array, which consists of M microphones with an interelement spacing of δ. If we attempt to steer the beamformer to angle θ. The steering vector of length M can be written as

$$\mathbf{d}(\omega,\theta) = \left[\begin{array}{cccc} 1 & e^{-\jmath\frac{\omega\delta}{c}\cos\theta} & \cdots & e^{-\jmath\frac{(M-1)\omega\delta}{c}\cos\theta} \end{array}\right]^T, \quad (1)$$

where $\jmath$ is the imaginary unit, $\omega = 2\pi f$ is the angular frequency, $f > 0$ is the temporal frequency, and the superscript ^{T} is the transpose operator.

Beamforming is performed by applying an appropriate complex spatial filter to the microphone array observations to recover the desired signal. An estimate of the desired signal in the frequency domain is obtained by

$$\begin{aligned} Z(\omega) &= \mathbf{h}^H(\omega)\,\mathbf{y}(\omega) \\ &= \mathbf{h}^H\mathbf{d}(\omega,\theta_0)\,X(\omega) + \mathbf{h}^H\mathbf{v}(\omega), \end{aligned} \quad (2)$$

where the superscript ^{H} is the conjugate transpose operator, $\mathbf{h}(\omega)$ is the beamforming filter of length M, $\mathbf{y}(\omega) =$

This work was supported in part by the Pazy Research Foundation, in part by ISF-NSFC joint research program Grants 2514/17 and 61761146001, in part by the National Key Research and Development Program of China under Grant No. 2018AAA0102200 and the Key Program of NSFC Grant 61831019.

$\left[\begin{array}{cccc} Y_1(\omega) & Y_2(\omega) & \cdots & Y_M(\omega) \end{array}\right]^T$ is the array observation vector of length M, $X(\omega)$ is the desired signal, θ_0 denotes the desired look direction and with a linear DMA we often assume $\theta_0 = 0^\circ$, $\mathbf{v}(\omega)$ is the received noise vector having a similar form of $\mathbf{y}(\omega)$. To ensure that the desired signal passes the beamforming filter without any distortion, the distortionless constraint is imposed, i.e.,

$$\mathbf{h}^H(\omega)\,\mathbf{d}(\omega,\theta_0) = 1. \tag{3}$$

There are three common measures to evaluate the performance of the beamformer: the beampattern, DF and WNG. The beampattern describes the sensitivity of the beamformer to plane waves from different directions, which is defined as [10]

$$\mathcal{B}[\mathbf{h}(\omega),\theta] = \mathbf{h}^H(\omega)\,\mathbf{d}(\omega,\theta). \tag{4}$$

For any beamforming filter, it is necessary to obtain the maximum response at the desired look direction, i.e.,

$$\mathcal{B}[\mathbf{h}(\omega),\theta_0] \leq 1, \forall \theta \neq \theta_0. \tag{5}$$

If the inequality in (5) holds, the beampattern is called an effective one. Otherwise, the beamformer may amplify unwanted signals, leading to further contamination of the desired signal of interest instead of enhancing it.

The DF evaluates how directive is the beampattern and is defined as the squared magnitude of the beampattern at the look direction divided by the averaged value over $\theta \in [0,\pi]$. Mathematically [10],

$$\begin{aligned}\mathcal{D}[\mathbf{h}(\omega)] &= \frac{|\mathcal{B}[\mathbf{h}(\omega),\theta_0]|^2}{\frac{1}{2}\int_0^\pi |\mathcal{B}[\mathbf{h}(\omega),\theta]|^2 \sin\theta d\theta} \\ &= \frac{\left|\mathbf{h}^H(\omega)\,\mathbf{d}(\omega,\theta_0)\right|^2}{\mathbf{h}^H(\omega)\,\mathbf{\Gamma}(\omega)\,\mathbf{h}(\omega)},\end{aligned} \tag{6}$$

where $\mathbf{\Gamma}(\omega)$ is a matrix of size $M \times M$ with the (i,j)th element being given by $[\mathbf{\Gamma}(\omega)]_{i,j} = \mathrm{sinc}[\omega(j-i)/c]$ and $\mathrm{sinc}(x) = \sin(x)/x$.

The WNG measures the robustness of the beamformer against the array imperfection such as the position error or self noise of the sensors, which is defined as [10]

$$\mathcal{W}[\mathbf{h}(\omega)] = \frac{\left|\mathbf{h}^H(\omega)\,\mathbf{d}(\omega,\theta_0)\right|^2}{\mathbf{h}^H(\omega)\,\mathbf{h}(\omega)}. \tag{7}$$

3. DIFFERENTIAL BEAMFORMING METHOD

Differential beamformers use closely spaced acoustic sensors to measure the spatial differentials of the sound pressure field, which can produce frequency-invariant beampatterns. Ideally, an Nth-order differential beamformer has a beampattern of the following form [23]

$$\mathcal{B}_N(\theta) = \sum_{n=0}^{N} a_{N,n}\cos^n\theta, \tag{8}$$

where $a_{N,n}, n = 0,1,2,\ldots,N$, are real coefficients, which determine the shape of the beampattern. For a linear DMA with the distortionless constraint given in (3), the coefficients should satisfy $\sum_{n=0}^{N} a_{N,n} = 1$.

Given the ideal beampattern in (8), the problem of differential beamforming can be converted as one of identifying a beamforming filter $\mathbf{h}(\omega)$ such that the resulting beampattern matches as close as possible the ideal beampattern. According to (8), the ideal, target differential beampattern has at most N distinct nulls, which are denoted as $\theta_{N,n}, n = 1,2,\ldots,N$. These nulls can be used to identify the beamforming filter [10]. Specifically, a linear system of $N+1$ equations can be constructed as following:

$$\mathbf{D}(\omega,\boldsymbol{\theta}_N)\,\mathbf{h}(\omega) = \mathbf{i}_{N+1}, \tag{9}$$

where $\mathbf{i}_{N+1}$ is a vector of length $N+1$ whose first element is 1 and all the other elements are 0, $\boldsymbol{\theta}_N = \left[\begin{array}{cccc} \theta_0 & \theta_{N,1} & \theta_{N,2} & \cdots & \theta_{N,N} \end{array}\right]^T$ is a vector of length $N+1$,

$$\mathbf{D}(\omega,\boldsymbol{\theta}_N) = \left[\begin{array}{c} \mathbf{d}^H(\omega,\theta_0) \\ \mathbf{d}^H(\omega,\theta_{N,1}) \\ \mathbf{d}^H(\omega,\theta_{N,2}) \\ \vdots \\ \mathbf{d}^H(\omega,\theta_{N,N}) \end{array}\right], \tag{10}$$

is the constraint matrix of size $(N+1)\times M$. Suppose that $M = N+1$, $\mathbf{D}$ is then a square matrix and the beamformer can be obtained by solving the following linear system

$$\mathbf{h}_{\mathrm{D}} = \mathbf{D}^{-1}(\omega,\boldsymbol{\theta}_N)\,\mathbf{i}_N, \tag{11}$$

where the subscript "$_{\mathrm{D}}$" stands for direct inverse.

Generally, the differential beamformer in (11) suffers from the problem of white noise amplification at low frequencies. One way to deal with this problem is through increasing the number of microphones while fixing the order of the differential beamformer. In this case, we have $M > N+1$ and $\mathbf{D}$ in (9) is no longer a square but a tall matrix. One can identify the beamforming filter through the minimum-norm method, i.e.,

$$\mathbf{h}_{\mathrm{MN}} = \mathbf{D}^H(\omega,\boldsymbol{\theta}_N)\left[\mathbf{D}(\omega,\boldsymbol{\theta}_N)\,\mathbf{D}^H(\omega,\boldsymbol{\theta}_N)\right]^{-1}\mathbf{i}_N. \tag{12}$$

With this minimum-norm beamformer, the more the microphones are used, the higher is the WNG.

4. PERFORMANCE ANALYSIS

In order to analyze the effect of nulls' positions on the DF, we rewrite the ideal differential beampattern in (8) as an explicit function of the null, θ_{n}, i.e.,

$$\mathcal{B}_{N,\theta_{\mathrm{n}}}(\theta) = \left(\sum_{n=0}^{N-1} b_{N,n}\cos^n\theta\right)(\cos\theta - \cos\theta_{\mathrm{n}}). \tag{13}$$

where $b_{N,n}, n = 0,1,\ldots,N-1$ are real coefficients. The relationship between the coefficients $a_{N,n}$ and $b_{N,n}$ can be derived as

$$\mathbf{a} = \mathbf{T}\mathbf{b}, \tag{14}$$

where

$$\mathbf{a} = \left[\begin{array}{cccc} a_{N,0} & a_{N,1} & \cdots & a_{N,N} \end{array}\right]^T, \tag{15}$$

$$\mathbf{b} = \left[\begin{array}{cccc} b_{N,0} & b_{N,1} & \cdots & b_{N,N-1} \end{array}\right]^T, \tag{16}$$

and

$$\mathbf{T} = \left[\begin{array}{ccccc} -\cos\theta_{\mathrm{n}} & & & & \\ 1 & -\cos\theta_{\mathrm{n}} & & & \\ & 1 & -\cos\theta_{\mathrm{n}} & & \\ & & \ddots & \ddots & \\ & & & 1 & -\cos\theta_{\mathrm{n}} \\ & & & & 1 \end{array}\right] \tag{17}$$

is a matrix of size $(N+1)\times N$. Then, the distortionless constraint becomes

$$\sum_{n=0}^{N-1} b_{N-1,n} = \frac{1}{1-\cos\theta_{\mathrm{n}}}. \tag{18}$$

According to [23], the DF of the Nth-order ideal differential beampattern can be written as

$$\begin{aligned}\mathcal{D}_N &= \frac{|\mathcal{B}_N(\theta_0)|^2}{\frac{1}{2}\int_0^{\pi}|\mathcal{B}_N(\theta)|^2\sin\theta d\theta}\\ &= \frac{1}{\mathbf{a}^T\mathbf{H}\mathbf{a}},\end{aligned} \tag{19}$$

where $\mathbf{H}$ is a Hankel matrix of size $(N+1)\times(N+1)$ whose (i,j)th element is given by

$$[\mathbf{H}]_{i,j} = \begin{cases} \frac{1}{i+j-1}, & i+j \text{ is even} \\ 0, & \text{otherwise} \end{cases}. \tag{20}$$

Submitting (14) into (19), the DF of the ideal differential beampattern with an explicit null, θ_{n}, is calculated as

$$\mathcal{D}_{N,\theta_{\mathrm{n}}} = \frac{1}{\mathbf{b}^T\overline{\mathbf{H}}\mathbf{b}}, \tag{21}$$

where

$$\overline{\mathbf{H}} = \mathbf{T}^T\mathbf{H}\mathbf{T}. \tag{22}$$

Considering the fact that it is real symmetrical, one can decompose the $\overline{\mathbf{H}}$ matrix as

$$\overline{\mathbf{H}} = \mathbf{U}\mathbf{\Lambda}\mathbf{U}^T, \tag{23}$$

where $\mathbf{U}$ is an orthogonal matrix of size $N\times N$, $\mathbf{\Lambda} = \mathrm{diag}(\lambda_1,\lambda_2,\ldots,\lambda_N)$ is a diagonal matrix of size $N\times N$ with its diagonal elements $\lambda_n, n=1,2,\ldots,N$, being the eigenvalues of $\overline{\mathbf{H}}$. It can be checked that $\overline{\mathbf{H}}$ is positive semi-definite. So, we have $\lambda_n \geq 0$.

Then, the denominator of the DF in (21) can be written as

$$\begin{aligned}\mathbf{b}^T\overline{\mathbf{H}}\mathbf{b} &= \mathrm{tr}\left(\mathbf{b}^T\overline{\mathbf{H}}\mathbf{b}\right)\\ &= \mathrm{tr}\left(\mathbf{U}^T\mathbf{b}\mathbf{b}^T\mathbf{U}\mathbf{\Lambda}\right)\\ &= \sum_{n=1}^{N}\lambda_n[\mathbf{K}]_{n,n},\end{aligned} \tag{24}$$

where $\mathrm{tr}(\cdot)$ denotes the trace of a matrix and $\mathbf{K} = \mathbf{U}^T\mathbf{b}\mathbf{b}^T\mathbf{U}$ with $[\mathbf{K}]_{n,n}$ being its (n,n)th element.

Denoting the minimal eigenvalue as $\lambda_{\min}$, we then have

$$\begin{aligned}\mathbf{b}^T\overline{\mathbf{H}}\mathbf{b} &\geq \lambda_{\min}\sum_{n=1}^{N}[\mathbf{K}]_{n,n}\\ &= \lambda_{\min}\mathrm{tr}(\mathbf{K})\\ &= \lambda_{\min}\mathrm{tr}\left(\mathbf{b}^T\mathbf{b}\right)\\ &\geq \frac{\lambda_{\min}}{N}\left(\sum_{n=0}^{N-1}b_{N,n}\right)^2\\ &= \frac{\lambda_{\min}}{N(1-\cos\theta_{\mathrm{n}})^2}.\end{aligned} \tag{25}$$

Therefore, one can conclude that for any order of DMA, when θ_{n} approaches 0° (the desired look angle), the denominator of DF, i.e., $\mathbf{b}^T\overline{\mathbf{H}}\mathbf{b}$ approaches infinite, which means that the DF is close to 0 (or minus infinite dB).

5. SIMULATIONS

In this section, we study the performance of the first- and second-order differential beamformers as a function of the nulls' positions in both anechoic and reverberant acoustic environments.

We consider a linear microphone array in a room of size $6\times5\times4$ m. A reference microphone is placed at (x_0,y_0,z_0). In order to reduce the impact of the reference point on evaluation, we performed 100 experiments for every evaluation and each time the reference point is randomly selected within the room. The averaged results are reported in this paper. For the first-order differential beamformer, two sensors are used, one at the reference point, the other at $(x_0-0.01,y_0,z_0)$, i.e., the spacing between the two sensors is 1 cm. For second-order differential beamformer, the spacing is again 1 cm and three sensors are used: one at the reference point, the other two at $(x_0-0.01,y_0,z_0)$ and $(x_0-0.02,y_0,z_0)$ respectively. A desired source placed at $(x_0+1.5,y_0,z_0)$. The room impulse response (RIR) from the source to each microphone is generated with the image model method [26,27]. The beamformers are implemented in the STFT domain. Specifically, the signals are partitioned into overlapping frames with a frame size of 256 points and an overlapping rate of 75%. For each frame, a Kaiser window is applied and the windowed frame signal is subsequently transformed into the STFT domain. After performing beamforming in each subband, the output is formed with overlap-add technique. All the source signals have the same sampling rate of 16 kHz.

We first measure the practical beampatterns of different differential beamformers in an anechoic environment, where the reflection coefficients of all the walls, ceiling and floor are set to 0. For each order of DMA, four differential beamformers with different nulls, i.e., $\theta_{\mathrm{n}}\in\{120^\circ,90^\circ,60^\circ,30^\circ\}$, are measured. Specifically, for the first-order DMA, we set $\theta_{1,1}=\theta_{\mathrm{n}}$ while for the second-order DMA, the two nulls are set to $\theta_{2,1}=165^\circ$ and $\theta_{2,2}=\theta_{\mathrm{n}}$ respectively. Then the beamformers to be measured are computed according to (11). To measure the beampattern, a narrowband source is placed in the horizontal plane, which moves in a circle with a radius of 1.5 m and the center at the reference point. In other words, the source's coordinates are $(x_{\mathrm{s}},y_{\mathrm{s}},z_0)$, where $x_{\mathrm{s}}=x_0+r_{\mathrm{s}}\cos\theta_{\mathrm{s}}$, $y_{\mathrm{s}}=y_0+r_{\mathrm{s}}\sin\theta_{\mathrm{s}}$, $\theta_{\mathrm{s}}\in\{0^\circ:1^\circ:360^\circ\}$, and $r_{\mathrm{s}}=1.5$ m. The source is a narrowband signal of 2 kHz. At each source position, the RIR from the source to the microphones are generated with the image model method [26,27]. The array observations are then obtained by convolving the source signal with the corresponding RIRs. The power of the beamformer's output is subsequently computed. Repeating this process for $\theta_{\mathrm{s}}\in\{0^\circ:1^\circ:360^\circ\}$ and normalizing all the results with respect to the value at the endfire position, we obtain the measured beampattern.

Then, we study the performance of different differential beamformers on interference suppression in reverberant environments (with reverberation time $T_{60}=150$ ms) as a function of interference incidence angle, which is measured by the signal-to-interference (SIR) gain (denoted as $\mathcal{G}_{\mathrm{SIR}}$) [28]. A desired source is placed at $(x_0+1.5,y_0,z_0)$ and an interference at $(x_{\mathrm{i}},y_{\mathrm{i}},z_0)$, where $x_{\mathrm{i}}=x_0+r_{\mathrm{i}}\cos\theta_{\mathrm{i}}$, $y_{\mathrm{i}}=y_0+r_{\mathrm{i}}\sin\theta_{\mathrm{i}}$, $\theta_{\mathrm{i}}\in\{20^\circ:10^\circ:180^\circ\}$, and $r_{\mathrm{i}}=1.5$ m. The desired and interference signals are both clean speech. For each position of interference, we set $\theta_{1,1}=\theta_{\mathrm{i}}$ and $\theta_{2,1}=165^\circ$ and $\theta_{2,2}=\theta_{\mathrm{i}}$ for the first- and second-order DMA, respectively, and compute the corresponding beamformer by (11) so that the beamformer always has a null towards the interference. After array signal generation and beamforming, we obtain the SIR gain for different interference incidence angles.

Figure 1 plots the designed and measured beampatterns of the

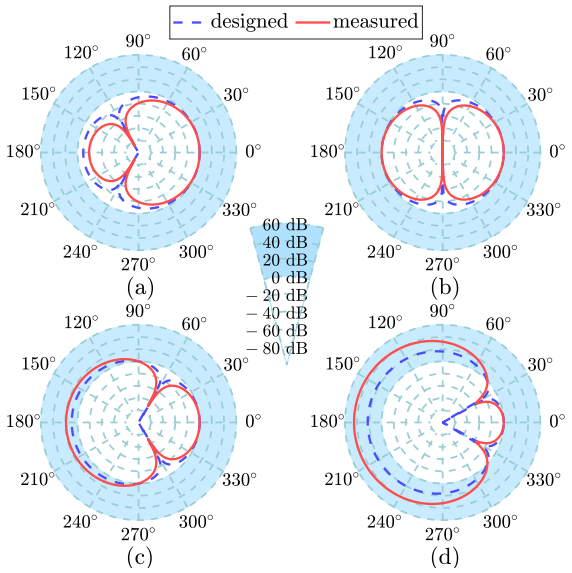

Fig. 1. Designed and measured beampatterns of the first-order DMA at $f = 2$ kHz: (a) $\theta_{\mathrm{n}} = 120°$, (b) $\theta_{\mathrm{n}} = 90°$, (c) $\theta_{\mathrm{n}} = 60°$, and (d) $\theta_{\mathrm{n}} = 30°$.

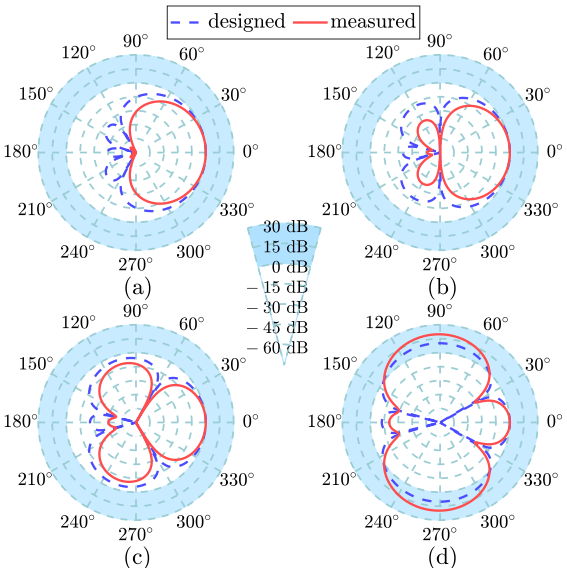

Fig. 3. Designed and measured beampatterns of the second-order DMA at $f = 2$ kHz: (a) $\theta_{\mathrm{n}} = 120°$, (b) $\theta_{\mathrm{n}} = 90°$, (c) $\theta_{\mathrm{n}} = 60°$, and (d) $\theta_{\mathrm{n}} = 30°$.

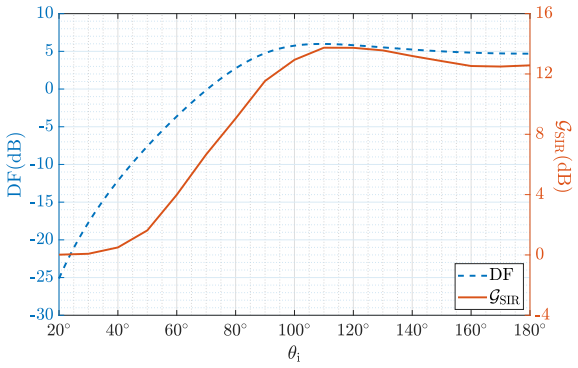

Fig. 2. DF and SIR gains as a function of the interference incidence angle, θ_{i}, for the first-order DMA.

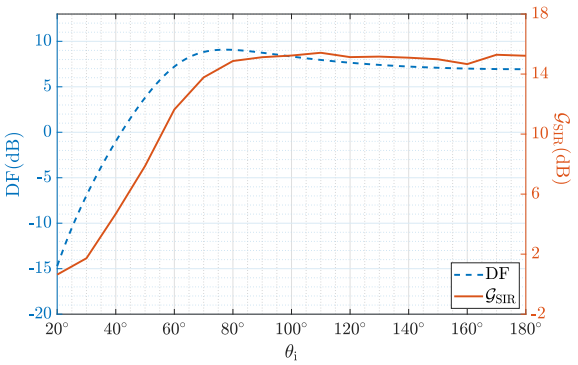

Fig. 4. DF and SIR gain as a function of the interference incidence angle, θ_{i}, for the second-order DMA.

first-order DMA for frequency, $f = 2$ kHz, and different $\theta_{\mathrm{n}} \in \{120°, 90°, 60°, 30°\}$. It is seen that the designed beamformer successfully formed a null at every specified direction, and the measured beampatterns matches well the designed ones. However, as the angle of null closer to 0 (i.e., the desired look direction), the null tends to be shallower, indicating a performance degradation

In Fig. 2, we plot the DF at $f = 2$ kHz and SIR gain of the first-order DMA, as a function of null angle, θ_{n}, in the left and right axis, respectively. It is seen that the DF is high for $\theta_{\mathrm{n}} \geq 90°$, and then decreases rapidly as the null direction moves closer to the desired look direction, which is consistent with the theoretical analysis. As for the SIR gain, is similar to the DF, i.e., the gain decreases as the interference is incident from a direction closer to $0°$.

Figures 3 and 4 plot the performance of the second-order DMA in the same condition. In Fig. 3, one can also see some degradation on beampattern effectiveness and null depth as the angle of the null decreases. Compared with Fig. 1, when $\theta_{\mathrm{n}} = 60°$, the beampattern of the first-order DMA is noneffective, while the beampattern of the second-order DMA is effective, which means that for the same angle of null, a higher order DMA can help to improve the effectiveness of the beampattern. It is also observed that the DF and SIR gains can keep a high value at first, but suffer from huge decline when $\theta_{\mathrm{n}} \leq 60°$, which means that compared with the first-order DMA, the second-order DMA can achieve a good performance in terms of DF and interference suppression for a larger range of interference incidence angles.

6. CONCLUSIONS

This paper studied the impact of the null directions on the performance of differential beamformers. A new analytical expression of ideal differential beampattern was first presented, which includes the information of a null explicitly. Based on this new form, we showed through theoretical analysis that as the null approaches to the desired look direction the DF decreases rapidly. We validated the performance analysis of the differential beamformer through simulations using the beampattern effectiveness, null depth, directivity factor, and SIR gain as the performance metrics. The results showed that properly setting the nulls positions is important for DMA design, which plays an important role on performance.

7. REFERENCES

[1] J. Benesty, J. Chen, and Y. Huang, *Microphone Array Signal Processing*. Berlin, Germany: Springer-Verlag, 2008.

[2] G. W. Elko and J. Meyer, "Microphone arrays," in *Springer Handbook of Speech Processing*, J. Benesty, M. M. Sondhi, and Y. Huang, Eds. Berlin, Germany: Springer-Verlag, 2008, ch. 48, pp. 1021–1041.

[3] H. Sun, S. Yan, and U. P. Svensson, "Robust spherical microphone array beamforming with multi-beam-multi-null steering, and sidelobe control," in *Proc. IEEE Workshop Appl. Signal Process. Audio Acoust.*, Oct. 2009, pp. 113–116.

[4] C. Li, J. Benesty, and J. Chen, "Beamforming based on null-steering with small spacing linear microphone arrays," *J. Acoust. Soc. Am.*, vol. 143, no. 5, pp. 2651–2665, May 2018.

[5] H. Schepker, L. T. Tran, S. Nordholm, and S. Doclo, "Acoustic feedback cancellation for a multi-microphone earpiece based on a null-steering beamformer," in *Proc. IEEE Int. Workshop Acoust. Signal Enhancement*, Set. 2016, pp. 1–5.

[6] H. L. Van Trees, *Optimum Array Processing: Part IV of Detection, Estimation, and Modulation Theory*. Hoboken, NJ, USA: Wiley, 2004.

[7] J. Benesty, I. Cohen, and J. Chen, *Fundamentals of Signal Enhancement and Array Signal Processing*. Hoboken, NJ, USA: Wiley, 2018.

[8] R. A. Monzingo and T. W. Miller, *Introduction to Adaptive Arrays*. Raleigh, NC, USA: SciTech., 2004.

[9] J. Li, Z. Wang, and P. Stoica, "Robust Capon beamforming," in *Robust Adaptive Beamforming*, J. Li and P. Stoica, Eds. Hoboken, NJ, USA: Wiley, 2005, ch. 3, pp. 91–200.

[10] J. Benesty and J. Chen, *Study and Design of Differential Microphone Arrays*. Berlin, Germany: Springer-Verlag, 2012.

[11] J. Benesty, J. Chen, and I. Cohen, *Design of Circular Differential Microphone Arrays*. Berlin, Germany: Springer-Verlag, 2015.

[12] X. Wu, H. Chen, J. Zhou, and T. Guo, "Study of the mainlobe misorientation of the first-order steerable differential array in the presence of microphone gain and phase errors," *IEEE Signal Process. Lett.*, vol. 21, no. 6, pp. 667–671, Jun. 2014.

[13] G. W. Elko and A.-T. N. Pong, "A steerable and variable first-order differential microphone array," in *Proc. IEEE Int. Conf. Acoust., Speech Signal Process.*, Apr. 1997, pp. 223–226.

[14] E. De Sena, H. Hacihabiboglu, and Z. Cvetkovic, "On the design and implementation of higher order differential microphones," *IEEE Trans. Audio, Speech, Lang. Process.*, vol. 20, no. 1, pp. 162–174, Jan. 2012.

[15] J. Byun, Y. C. Park, and S. W. Park, "Continuously steerable second-order differential microphone arrays," *J. Acoust. Soc. Am.*, vol. 143, no. 3, pp. EL225–EL230, Mar. 2018.

[16] F. Borra, A. Bernardini, F. Antonacci, and A. Sarti, "Efficient implementations of first-order steerable differential microphone arrays with arbitrary planar geometry," *IEEE/ACM Trans. Audio, Speech, Lang. Process.*, vol. 28, pp. 1755–1766, May 2020.

[17] A. Bernardini, M. DAria, R. Sannino, and A. Sarti, "Efficient continuous beam steering for planar arrays of differential microphones," *IEEE Signal Process. Lett.*, vol. 24, no. 6, pp. 794–798, Jun. 2017.

[18] H. Teutsch and G. W. Elko, "First- and second-order adaptive differential microphone arrays," in *Proc. IEEE Int. Workshop Acoust. Signal Enhancement*, Sep. 2001, pp. 1–5.

[19] F. Borra, A. Bernardini, F. Antonacci, and A. Sarti, "Uniform linear arrays of first-order steerable differential microphones," *IEEE/ACM Trans. Audio, Speech, Lang. Process.*, vol. 27, no. 12, pp. 1906–1918, Dec. 2019.

[20] G. Huang, J. Benesty, I. Cohen, and J. Chen, "A simple theory and new method of differential beamforming with uniform linear microphone arrays," *IEEE/ACM Trans. Audio, Speech, Lang. Process.*, vol. 28, pp. 1079–1093, Mar. 2020.

[21] G. W. Elko, "Differential microphone arrays," in *Audio Signal Processing for Next-Generation Multimedia Communication Systems*, Y. Huang and J. Benesty, Eds. Berlin, Germany: Springer,, 2004, ch. 2, pp. 11–65.

[22] J. Chen, J. Benesty, and C. Pan, "On the design and implementation of linear differential microphone arrays," *J. Acoust. Soc. Am.*, vol. 136, no. 6, pp. 3097–3113, Dec. 2014.

[23] G. W. Elko, "Superdirectional microphone arrays," in *Acoustic Signal Processing for Telecommunication*, S. L. Gay and J. Benesty, Eds. Berlin, Germany: Springer, 2000, ch. 10, pp. 181–237.

[24] C. Pan, J. Benesty, and J. Chen, "Design of directivity patterns with a unique null of maximum multiplicity," *IEEE/ACM Trans. Audio, Speech, Lang. Process.*, vol. 24, no. 2, pp. 226–235, Feb. 2016.

[25] G. Huang, I. Cohen, J. Chen, and J. Benesty, "Continuously steerable differential beamformers with null constraints for circular microphone arrays," *J. Acoust. Soc. Am.*, vol. 148, no. 3, pp. 1248–1258, Sep. 2020.

[26] J. B. Allen and D. A. Berkley, "Image method for efficiently simulating small-room acoustics," *J. Acoust. Soc. Am.*, vol. 65, no. 4, pp. 943–950, Apr. 1979.

[27] P. M. Peterson, "Simulating the response of multiple microphones to a single acoustic source in a reverberant room," *J. Acoust. Soc. Am.*, vol. 80, no. 5, pp. 1527–1529, Nov. 1986.

[28] M. Souden, J. Benesty, and S. Affes, "A study of the LCMV and MVDR noise reduction filters," *IEEE Trans. Signal Process.*, vol. 58, no. 9, pp. 4925–4935, Sep. 2010.